

Study on switched reluctance generator^{*}

PAN Zai-ping (潘再平)[†], JIN Ying (金英), ZHANG Hui (张慧)

(College of Electrical Engineering, Zhejiang University, Hangzhou 310027, China)

[†]E-mail: panzaiping@zju.edu.cn

Received Aug. 8, 2003; revision accepted Sept. 15, 2003

Abstract: The linear and non-linear math models of the switched reluctance generator (SRG) in generator mode were established in this work. The phase current and energy conversion process during generator operation were simulated by the linear math model. The non-linear math model was used to analyze the characteristics of the SRG operation in self-excitation mode and in separately-excitation mode. Some important findings on how the SRG is operated and controlled were obtained in this study, which provides theoretical basis for further design and experimental study.

Key words: SRG, Inductance, Power analysis, Math model, Simulation, Exciting mode

Document code: A

CLC number: TM352

INTRODUCTION

Wind energy, being a clean, renewable source of energy has been used for centuries. Various schemes for generating electricity from the wind had been proposed (Rim and Krishnan, 1994; Pan, 1993). The SRG's attributes which make it ideally suited for wind energy systems include extreme robustness, high efficiency of energy conversion, ability to work over very large speed ranges, high energy density, and control simplicity. It has shown great developing potential and study value in the area of wind power generation (Cardenas *et al.*, 1995; Torrey, 2002).

Ordinarily, the structure of SRG is double protruding pole. The SRG in Fig.1 has steel laminations on the rotor and stator. There are no windings or permanent magnets on the rotor, and there are concentrated windings placed around each salient pole on the stator. The coils around the in-

dividual poles are connected to form the phase windings.

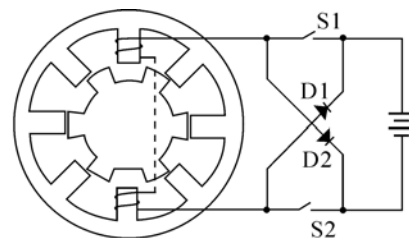


Fig.1 Sketch of SRG

The SRG has two phases (excitation and generation) in one electrifying period, with generation being the primary phase. When the two switches, S1 and S2, are turned on, the windings on the stator are excited by the outer circuit, and the electrical energy and mechanical energy provided by exterior circuit are converted into magnetic field energy. When the two switches are turned off and the two diodes, D1 and D2, are turned on, the magnetic field energy and mechanical energy are converted into electricity energy feeding back to the source or supplying power to the load. Because of the char-

^{*} Project (No. 599072) supported by the Natural Science Foundation of Zhejiang Province, China.

acteristics of time-sharing excitation, the control of SRG is very flexible. And there are several parameters for controlling SRG, such as turn-on angle, turn-off angle, and exciting voltage and controlling mode, all these will affect the generation greatly.

LINEAR MATH MODEL OF SRG AND ENERGY ANALYSIS

Linear math model

Fig.2 shows the variation of inductance with rotor position for one phase winding, idealized in that magnetic saturation, and the ‘rounding’ effect of the fringing fields are neglected (Miller *et al.*, 1990). According to the above suppositions, the math model of SRG is ideal and linear.

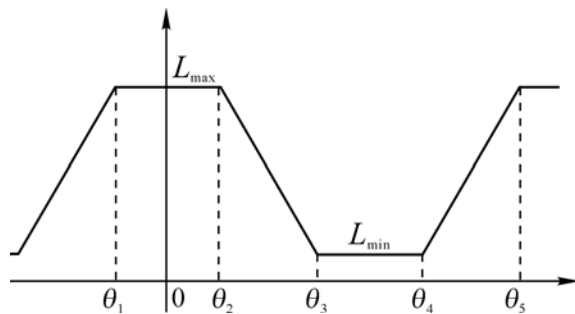


Fig.2 The relationship between inductance and the position of the rotor in ideal and linear math model

The iron cores of the stator and the rotor in SRG are all protruding poles. The distribution of the magnetic field is different when the relative position between rotor pole and the electrified phase on the stator is different. So the winding inductance L will change along with the change of the relative position between rotor pole and stator pole. When the rotor is turning, the inductance of windings will change from the maximum L_{max} to the minimum L_{min} periodically. The inductance reaches maximum when the axes of rotor pole and stator pole are in the same position and reaches minimum when the axis of the rotor pole and the center of the stator pole are in the same position. The relationship between inductance $L(\theta)$ and the position of the rotor θ can be shown through the following function (Chen *et al.*, 2001):

$$L(\theta) = \begin{cases} L_{max} - K(\theta_1 - \theta) & \theta_{on} \leq \theta < \theta_1 \\ L_{max} & \theta_1 \leq \theta < \theta_2 \\ L_{max} - K(\theta - \theta_2) & \theta_2 \leq \theta < \theta_3 \\ L_{min} & \theta_3 \leq \theta < \theta_4 \\ L_{min} - K(\theta - \theta_4) & \theta_4 \leq \theta < \theta_5 \end{cases} \quad (1)$$

Among the functions, θ_{on} is the turn-on angle, $K = (L_{max} - L_{min}) / (\theta_3 - \theta_2)$.

Suppose $\theta_{on} \leq \theta_1$, $\theta_2 \leq \theta_{off} \leq \theta_3$, $\theta_4 \leq (2\theta_{off} - \theta_{on}) \leq \theta_5$. The change of phase current can be divided into six phases: (1) Starting phase ($\theta_{on} \leq \theta \leq \theta_1$); (2) Rising linearly phase ($\theta_1 \leq \theta \leq \theta_2$); (3) Rising continuously phase ($\theta_2 \leq \theta \leq \theta_{off}$); (4) Generating phase ($\theta_{off} \leq \theta \leq \theta_3$); (5) Falling linearly phase ($\theta_3 \leq \theta \leq \theta_4$); (6) Falling continuously phase ($\theta_4 \leq \theta \leq \theta_5$).

The six phases of the phase current’s change can be shown by the uniform function below (Zhang and Pan, 2003):

$$i(\theta) = \begin{cases} \frac{u}{\omega L(\theta)}(\theta - \theta_{on}) & \theta_{on} \leq \theta < \theta_{off} \\ \frac{u}{\omega L(\theta)}(2\theta_{off} - \theta_{on} - \theta) & \theta_{off} \leq \theta < (2\theta_{off} - \theta_{on}) \end{cases} \quad (2)$$

Because $\psi(\theta) = L(\theta)i(\theta)$, the analytic function of the flux can be obtained as:

$$\psi(\theta) = \begin{cases} \frac{u}{\omega}(\theta - \theta_{on}) & \theta_{on} \leq \theta < \theta_{off} \\ \frac{u}{\omega}(2\theta_{off} - \theta_{on} - \theta) & \theta_{off} \leq \theta < (2\theta_{off} - \theta_{on}) \end{cases} \quad (3)$$

Analysis of energy

Neglecting the resistance loss, medium loss and mechanical loss, the following equation can be obtained:

$$\pm ui = Li \frac{di}{dt} + i^2 \frac{dL}{d\theta} \omega \quad (4)$$

For generating state, the input electrical energy and the output mechanical energy are all negative, which means mechanical energy is converted into electrical energy. Based on the linear

math models of phase current and flux established above, the change of magnetic field energy state can be drawn as shown in Fig.3. The turn-on angle in Fig.3, $\theta_{on}=\theta_1$, and the process of the magnetic field energy's variation in one period can be seen very clearly in the figure. When the primary switch is turned on, magnetic field energy in the system increases from zero and comes back to zero after one period. The change of magnetic field energy in one period is zero, and magnetic field just act as medium in the whole energy changing process. Thereby, the variation of mechanical energy and electrical energy in one period can be known through reviewing the variation of the magnetic field energy.

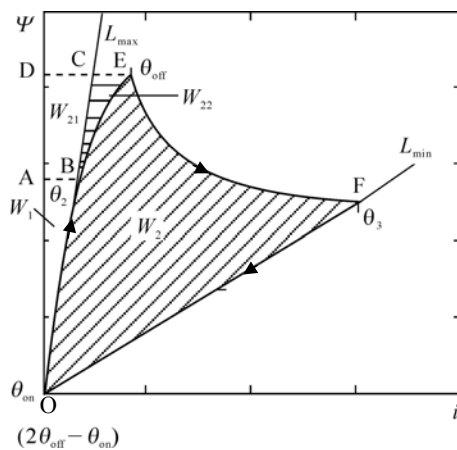


Fig.3 The change of magnetic field energy state

As shown in Fig.3, electrical source electrifies from θ_{on} to θ_{off} in one period. From θ_1 to θ_2 , the whole input electrical energy from the source is converted into magnetic field energy W_1 and stored in the magnetic field because $dL/d\theta=0$, and its magnitude is equal to the area of OAB. From θ_2 to θ_{off} , the input electrical energy from the source W_{21} (the area of ABCD) and the mechanical energy W_{22} (the area of BCE) are converted into magnetic field energy because $dL/d\theta<0$. The switches close at θ_{off} , and there is no input of the energy from the source and the phase current attenuate to zero at $2\theta_{off}-\theta_{on}$. In this process, from θ_{off} to θ_3 , $dL/d\theta<0$, the mechanical energy is converted into magnetic field energy constantly; From θ_3 to $2\theta_{off}-\theta_{on}$, $dL/d\theta=0$, there is

no input of mechanical energy and all the magnetic field energy is converted into electrical energy for output, which is shown as W_2 (the area of OBFEFO) in Fig.3. Thereby, the whole magnetic field energy converted from mechanical energy in one period is W_2+W_{22} , which is the effective electromagnetic energy (the area of OBCEFO). Enhancing the generating ability of the generator should start with enhancing the effective electromagnetic energy.

The way for enhancing the effective electromagnetic energy, should be considered in two parts below:

(1) With increasing the maximum inductance or decreasing the minimum inductance, the area of W_2+W_{22} will be increased. In order to achieve this purpose, the framework of SRG should be designed reasonably.

(2) The main way to improve the generation ability is to adjust the turn-on and turn-off angle. Remarkable effect can be obtained, if reasonable controlling strategy is chosen. Fig.4 shows the variation tendency of the magnetic field energy, when the turn-on and turn-off angle are varied. The effective area of magnetic field energy will increase along with the decrease of turn-on angle, which is shown in Fig.4a. The magnitude of current and the effective area of magnetic field energy will increase along with the increase of turn-off angle. Compared with the turn-on angle, the increase of effective magnetic field energy through changing turn-off angle is more remarkable.

NON-LINEAR INDUCTANCE MODEL OF SRG

The linear math model discussed above is very useful for basic characteristic's analysis of SRG, but is not suitable for quantitative analysis. In order to resolve this problem, the non-linear model should be considered.

Non-linear inductance model is based on the Fourier series of inductance. Normally, the former four times harmonic can satisfy the engineering computation requirement.

Supposing the inductance of SRG is $L(\theta,i)$, with $L(\theta,i)$ being a constant and periodic function

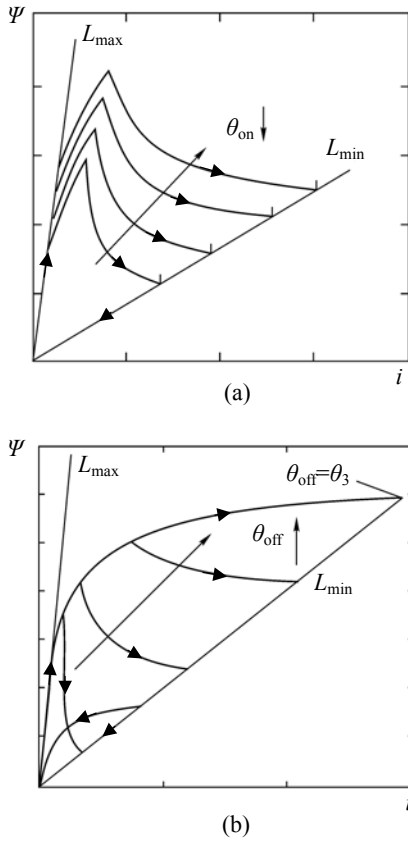


Fig.4 The relationship between magnetic field energy and turn-on, turn-off angle
 (a) The change of turn-on angle; (b) The change of turn-off angle

whose period is $T=2\pi/p_r$, where p_r is the number of rotor poles. The inductance, $L(\theta,i)$, can be expressed by the Fourier series:

$$L(\theta,i) = L_0(i) + \sum_{n=1}^{\infty} [L_{n1}(i) \cos np_r \theta + L_{n2}(i) \sin np_r \theta] \quad (5)$$

where

$$\begin{cases} L_{n1}(i) = \frac{p_r}{\pi} \int_{-\frac{\pi}{p_r}}^{\frac{\pi}{p_r}} L(\theta,i) \cos np_r \theta d\theta & (n=0, 1, 2, \dots) \\ L_{n2}(i) = \frac{p_r}{\pi} \int_{-\frac{\pi}{p_r}}^{\frac{\pi}{p_r}} L(\theta,i) \sin np_r \theta d\theta & (n=1, 2, 3, \dots) \end{cases}$$

When the mutual inductance is omitted, the inductance, $L(\theta,i)$, is symmetrical about the y-axis in the section of $[-\pi/p_r, \pi/p_r]$. Therefore, it is known

that $L_{n2}=0$, the Fourier series expression of inductance can be written as shown below:

$$L(\theta,i) = L_0(i) + \sum_{n=1}^{\infty} L_n(i) \cos np_r \theta \quad (6)$$

Omitting fifth and higher harmonics, the function can be written as:

$$L(\theta,i) = L_0(i) + L_1(i) \cos p_r \theta + L_2(i) \cos 2p_r \theta + L_3(i) \cos 3p_r \theta + L_4(i) \cos 4p_r \theta \quad (7)$$

The four unknown coefficients in the function can be derived from the four inductances known already, and they are the maximum inductance, $L_a(i) = L(0,i)$, the minimum inductance, $L_u(i) = L(\pi/p_r,i)$, the inductance at the 1/2 position, $L_m(i) = L(\pi/2p_r,i)$ and inductance at the 1/3 position, $L_t(i) = L(\pi/3p_r,i)$. The inductances at the 1/2 and 1/3 positions are related to the distance between the maximum and the minimum inductance. The four coefficients can be expressed as:

$$\begin{cases} L_0(i) = \frac{1}{4} [L_a(i) + L_u(i)] + \frac{1}{2} L_m(i) \\ L_1(i) = \frac{1}{4} L_a(i) - \frac{1}{2} L_m(i) + \frac{2}{3} L_t(i) - \frac{5}{12} L_u(i) \\ L_2(i) = \frac{1}{4} [L_a(i) + L_m(i)] - \frac{1}{2} L_u(i) \\ L_3(i) = \frac{1}{4} L_a(i) + \frac{1}{2} L_m(i) - \frac{2}{3} L_t(i) - \frac{1}{12} L_u(i) \end{cases} \quad (8)$$

The relationship between the position of rotor and inductance and current can be obtained accurately. The SRG experimented on was a four-phase motor having 8 stator poles and 6 rotor poles. Fig.5 shows rotor position vs calculated and measured flux for different currents. The two curves in the Fig.5 accorded well, especially near the rated current (7A–11A). The precision could satisfy project requirements.

The inductance model established above is the discrete curve of current. Inserting values must be used in practice, which go against real-time control. From the shape of the current in Fig.5, the continu-

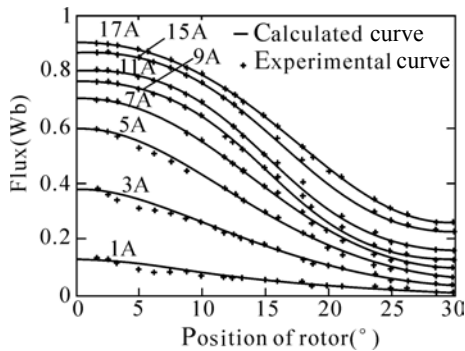


Fig.5 Rotor position vs flux calculated and flux measured for different currents

ous function of inductance vs current and rotor position can be found through several sets of second-degree polynomials which can also be used further theoretical research and system control of the SRG.

MODE OF EXCITATION OF SRG

SRG can be operated as either separately excited or self-excited (Abouzeid, 1998; Li et al., 2000). In the self-excited SRG, the initial excitation is supplied by an external voltage source. When generated voltage reaches steady value for control, the external source is cut off. Then excitation will be supplied by the voltage produced by the SRG itself. In this mode, the system volume is very small and the efficiency is high, because there is no outer source when the voltage is established. In the separately-excited SRG, the loop of excitation is independent of the generation, and the circuitry is complex. But because excitation is supplied by an external source during the whole running process of the SRG, there is no relationship between exciting voltage and output voltage at that time and the two voltages can be adjusted independently. Therefore, the control of separate excitation is convenient.

Self-excitation

Take phase A as example. In Fig.6, when the switches, S1 and S2, are turned on, capacitance C, supplies current to excite the windings of phase A and electrifies the load at the same time. When the

switches are turned off, the current in phase A flows through D1 and D2. The current in the windings keeps its direction, but the direction of the bus current is changed. The bus current electrifies capacitance C, and also electrifies the load. The SRG illustrated is a four-phase 8 stator poles, 6 rotor poles motor on which the non-linear model of the SRG was established. It is convenient if θ is selected as independent variable.

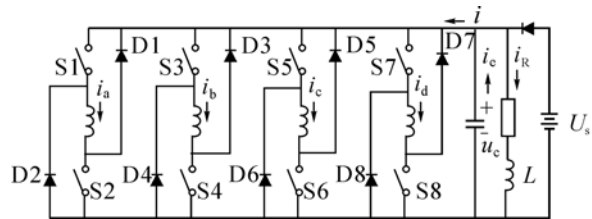


Fig.6 Main circuit of self-excitation generation strategy

The relationship between phase current and phase voltage is:

$$\begin{aligned} \pm u_c(\theta) = & i_a(\theta)r_a + \{L_a[\theta, i_a(\theta)] \\ & + \frac{\partial L_a[\theta, i_a(\theta)]}{\partial i_a(\theta)} i_a(\theta)\} \frac{di_a(\theta)}{dt} \omega \\ & + i_a(\theta) \frac{\partial L_a[\theta, i_a(\theta)]}{\partial \theta} \omega \end{aligned} \tag{9}$$

In this equation, the sign is positive when the switches, S1 and S2, are turned on, namely $\theta_{on} \leq \theta \leq \theta_{off}$. The sign is negative when the switches are turned off, namely $\theta \geq \theta_{off}$. The resistance of one phase winding in the motor is r_a . The relationship between other phase currents and voltages can be obtained based on the same principle.

The relationship between the voltage and the current in the load is:

$$L \frac{di_R(\theta)}{d\theta} + \frac{i_R(\theta)R}{\omega} = \frac{u_c(\theta)}{\omega} \tag{10}$$

The relationship between the voltage and the current in the bus is:

$$\frac{du_c(\theta)}{d\theta} = -[i(\theta) + i_R(\theta)]/(\omega C) \tag{11}$$

The bus current is $i(\theta)$.

Excitation and generation in SRG are at different time. It is necessary to construct a switch function to distinguish the two states, if uniform math model is to be established. Switch function, S_n ($n=1,2,3,4$), is introduced to show this relation in the four phases, A, B, C, D, respectively. The value is 1 when the phase related, and -1 if not. That is:

$$S_n = \begin{cases} 1, & \theta_{onn} \leq \theta \leq \theta_{offn} \\ -1, & \theta \geq \theta_{offn} \end{cases} \quad (n=1, 2, 3, 4) \quad (12)$$

The relationship between bus current and phase current is:

$$i(\theta) = S_1 i_a(\theta) + S_2 i_b(\theta) + S_3 i_c(\theta) + S_4 i_d(\theta) \quad (13)$$

Actually, the SRG bus current is the resultant of the four-phase current.

Take phase current, load current, and capacitance voltage of each phase as state variables and into the state equation of self-excitation as written below:

$$\begin{bmatrix} \dot{i}_a \\ \dot{i}_b \\ \dot{i}_c \\ \dot{i}_d \\ \dot{i}_R \\ \dot{u}_c \end{bmatrix} = \begin{bmatrix} A_i & 0 & 0 & 0 & 0 & A_u \\ 0 & B_i & 0 & 0 & 0 & B_u \\ 0 & 0 & C_i & 0 & 0 & C_u \\ 0 & 0 & 0 & D_i & 0 & D_u \\ 0 & 0 & 0 & 0 & -\frac{R}{\omega L} & \frac{1}{\omega L} \\ -\frac{S_1}{\omega C} & -\frac{S_2}{\omega C} & -\frac{S_3}{\omega C} & -\frac{S_4}{\omega C} & -\frac{1}{\omega C} & 0 \end{bmatrix} \begin{bmatrix} i_a \\ i_b \\ i_c \\ i_d \\ i_R \\ u_c \end{bmatrix} \quad (14)$$

where

$$A_i = -\frac{r_a + \frac{\partial L_a}{\partial \theta}}{L_a + \frac{\partial L_a}{\partial i_a} i_a}, A_u = -\frac{S_1}{\omega(L_a + \frac{\partial L_a}{\partial i_a} i_a)}$$

The coefficients of other phases are similar to those of phase A.

Separate-excitation

In Fig.7, U_s is the source for excitation and

capacitance C , is for storing energy and stabilizing voltage. Separate-excitation is different from self-excitation, and the loop of excitation (source for excitation, $U_s \rightarrow$ switch 1 \rightarrow windings in motor \rightarrow switch 2 $\rightarrow U_s$) and the loop of generation (windings in motor \rightarrow freewheeling diode 1 \rightarrow capacitance C and load \rightarrow freewheeling diode 2 \rightarrow windings in motor) are independent of each other, so the math model and characteristic are different from those of self-excitation. Take phase A as example. When the switches, S1 and S2, are turned on, the windings of phase A are excited by source U_s . When the switches are turned off, the current of phase A flows through D1 and D2, and electrifies capacitance C at the same time, and supply power to the load.

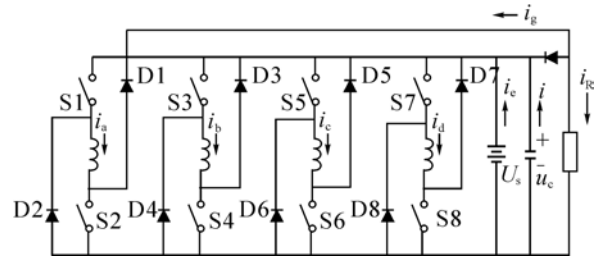


Fig.7 Main circuit for the separate-excitation generation strategy

The relationship between phase voltage and phase current is described below:

(1) The state of excitation ($\theta_{on} \leq \theta \leq \theta_{off}$) in the section affected when the switches are turned on is

$$U_s = i_a(\theta)r_a + \{L_a[\theta, i_a(\theta)] + \frac{\partial L_a[\theta, i_a(\theta)]}{\partial i_a(\theta)} i_a(\theta)\} \frac{di_a(\theta)}{dt} \omega + i_a(t) \frac{\partial L_a[\theta, i_a(\theta)]}{\partial \theta} \omega \quad (15)$$

(2) The state of electricity generation ($\theta \geq \theta_{off}$) in the section affected when the switches are turned off is

$$-u_c(\theta) = i_a(\theta)r_a + \{L_a[\theta, i_a(\theta)] + \frac{\partial L_a[\theta, i_a(\theta)]}{\partial i_a(\theta)} i_a(\theta)\} \frac{di_a(\theta)}{dt} \omega$$

$$+ i_a(t) \frac{\partial L_a[\theta, i_a(\theta)]}{\partial \theta} \omega \quad (16)$$

The relationship between the load voltage and load current is

$$L \frac{di_R(\theta)}{d\theta} + \frac{i_R(\theta)R}{\omega} = \frac{u_c(\theta)}{\omega} \quad (17)$$

The relationship between the voltage and the current in generating bus is

$$\frac{du_c(\theta)}{d\theta} = -[i_g(t) + i_R(t)]/(\omega C) \quad (18)$$

$i_g(\theta)$ is determined by generating current and has no relation to exciting current.

The loop of excitation and the loop of generation in the separately excited SRG are independent, so the loop of the excitation's switching characteristics can be described by the switch function S_n ; and the loop of generation's characteristic can be described by the function $(1-S_n)$.

$$S_n = \begin{cases} 1, & \theta_{onn} \leq \theta \leq \theta_{offn} \\ 0, & \theta \geq \theta_{offn} \end{cases} \quad (n=1, 2, 3, 4) \quad (19)$$

$$(1-S_n) = \begin{cases} 0, & \theta_{onn} \leq \theta \leq \theta_{offn} \\ -1, & \theta \geq \theta_{offn} \end{cases} \quad (n=1, 2, 3, 4) \quad (20)$$

The relationship between bus current and phase current is described below.

(1) There is current in the loop of excitation, just when the switches are turned on, so:

$$i_c(\theta) = S_1 i_a(i) + S_2 i_b(i) + S_3 i_c(i) + S_4 i_d(i) \quad (21)$$

(2) There is current in the loop of generation, so:

$$i_g(\theta) = (1-S_1)i_a(i) + (1-S_2)i_b(i) + (1-S_3)i_c(i) + (1-S_4)i_d(i) \quad (22)$$

Take phase current and exciting voltage, U_s and capacitance's voltage U_c of each phase as state variables and link the above functions. Then the

state equation of self-excitation can be written as shown below:

$$\begin{bmatrix} \dot{i}_a & \dot{i}_b & \dot{i}_c & \dot{i}_d & \dot{i}_R & \dot{u} & \dot{u}_c \end{bmatrix}^T = \begin{bmatrix} A_i & 0 & 0 & 0 & 0 & A_u S_1 & A_u(1-S_1) \\ 0 & B_i & 0 & 0 & 0 & B_u S_2 & B_u(1-S_2) \\ 0 & 0 & C_i & 0 & 0 & C_u S_3 & C_u(1-S_3) \\ 0 & 0 & 0 & D_i & 0 & D_u S_4 & D_u(1-S_4) \\ 0 & 0 & 0 & 0 & -\frac{R}{\omega L} & 0 & \frac{1}{\omega L} \\ 0 & 0 & 0 & 0 & 0 & 0 & 0 \\ -\frac{1-S_1}{\omega C} & -\frac{1-S_2}{\omega C} & -\frac{1-S_3}{\omega C} & -\frac{1-S_4}{\omega C} & -\frac{1}{\omega C} & 0 & 0 \end{bmatrix} \cdot \begin{bmatrix} i_a & i_b & i_c & i_d & i_R & u & u_c \end{bmatrix}^T \quad (23)$$

where the parameters, A_i , B_i , C_i , D_i , A_u , B_u , C_u and D_u are similar to those of self-excitation.

Simulation

The SRG simulated with the non-linear math model established above was a four-phase motor with 8 stator poles and 6 rotor poles. Fig.8 shows the simulated waves of self-excitation at different initial exciting voltage of $U_s=10$ V and $U_s=50$ V, when SRG reached steady speed of 750 r/min. The optimized switch angles were: turn-on angle $a_{on}=-15^\circ$, turn-off angle $a_{off}=15^\circ$, and the load was $R=50 \Omega$, $L=1$ mH.

Fig.8 shows that the SRG has the self-excitation ability. The steady state the generator finally reached was not related with initial exciting voltage but related with the time when the generator reached steady state. When the initial exciting voltage was 10 V, SRG reached steady state after around six periods (one period equal to 60° , mechanical angle); moreover, when initial exciting voltage was 50 V, the time was about five periods.

Simulation was done with the same generator which was this time separately excited under the same working condition. Exciting voltage was 10 V in Fig.9. The voltage's waves of the capacitance connected across the main circuit at different initial capacitance's voltages are also shown in this figure.

The analysis results showed that the steady state had no relation with the initial voltage of the

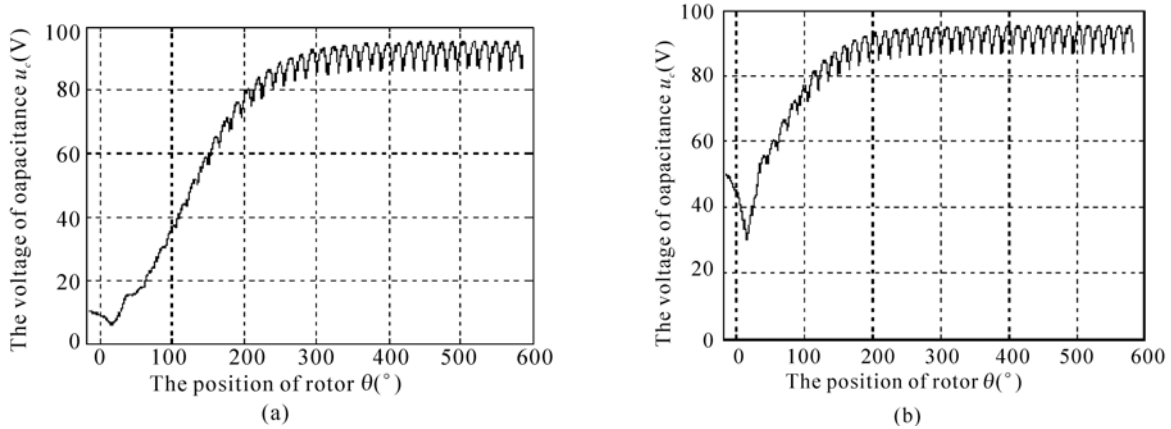


Fig.8 The wave of capacitance's voltage in self-excitation
 (a) Initial exciting voltage of 10 V; (b) Initial exciting voltage of 50 V

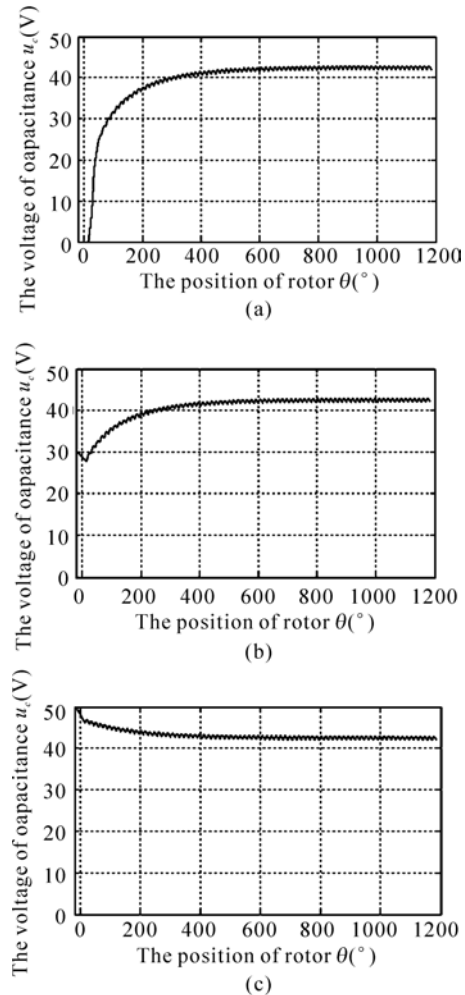


Fig.9 The wave of capacitance's voltage in separately excited SRG
 (a) $U_s=10$ V and $U_{c0}=0$ V; (b) $U_s=10$ V and $U_{c0}=30$ V; (c) $U_s=10$ V and $U_{c0}=50$ V

capacitance parallel connected on the main circuit, but had relation with the external exciting voltage. It can be seen in Fig.9 that though the time when SRG reached steady state became shorter and shorter with the increase of the initial capacitance voltage, the voltage of load remained the same after the generator reached steady state finally. Even when the initial capacitance voltage was higher than the steady state voltage, the result was the same.

Fig.10 (see the next page) shows the simulated waves of phase A current at the initial moment of generation. The large magnitude instantaneous peak current that occurred at the initial moment of generation is harmful to the SRG controller. When exciting voltage was 10 V and initial capacitance voltage was 0 V, the large magnitude peak current occurred in phase A during the initial period was three to four times the normal current by reason that the initial capacitance voltage was 10 V, then the peak current at the first period reduced to 1/2. In Fig.10c, the capacitance voltage was 30 V, then the peak current at the first period became normal on the whole.

CONCLUSION

This research established the linear and non-linear math model of SRG. The SRG linear math model was used to simulate and analyze the phase

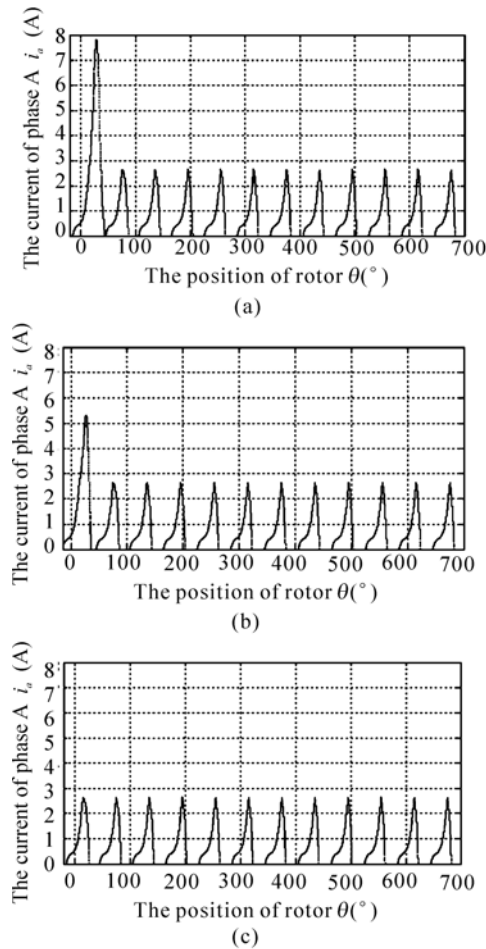


Fig.10 The waveform of A-phase current

(a) $U_s=10$ V and $U_{c0}=0$ V; (b) $U_s=10$ V and $U_{c0}=10$ V; (c) $U_s=10$ V and $U_{c0}=30$ V

current and the energy conversion process during generation, and find ways to enhance the generating ability of SRG. The non-linear math model of the SRG was used to simulate and analyze the operating characteristic in the two exciting modes (self-excitation and separate-excitation) and obtain some useful conclusions on the operating and controlling

characteristic of SRG. Theoretical analysis and computer simulation showed the correctness of the linear and non-linear math model of SRG.

References

- Abouzeid, M., 1998. Load Effect on the Output Current Generated from the Switched Reluctance Generator. *In: Proceedings of Seventh International Conference on Power Electronics and Variable Speed Drives*, London, UK, p.560-567.
- Cardenas, R., Ray, W.F., Asher, G.M., 1995. Switched Reluctance Generators for Wind Energy Applications. *In: Proceedings of Power Electronics Specialists Conference, PESC'95*, Atlanta, USA, 1:559-564.
- Chen, H., Mang, C., Zhao, X., 2001. Research on the Switched Reluctance Wind Generator System. *In: Proceedings of IEEE International Conference on Systems, Man, and Cybernetics*, Tucson, AZ, USA, 3:1936-1941.
- Li, S.J., Li, Q., Lu, G., Ma, R.Q., 2000. Switched reluctance generator self-exciting mechanism. *Micromotors*, 33 (5):10-11, 45 (in Chinese).
- Miller, T.J.E., Stephenson, J.M., MacMinn, S.R., Hendershot, J.R., 1990. Switched Reluctance Drives. *In: IEEE Tutorial, IEEE 25th IAS Annual Meeting*, Seattle, WA, USA.
- Pan, Z.P., 1993. Variable speed and constant frequency technology in wind electricity generation. *Energy Engineering*, (2):18-22(in Chinese).
- Rim, G., Krishnan, R., 1994. Variable Speed Constant Frequency Power Conversion with A Switched Reluctance Machine. *In: Proceedings of Applied Power Electronics Conference, APEC'94*, Orlando, FL, USA, 1:63-71.
- Torrey, D.A., 2002. Switched reluctance generators and their control. *IEEE Trans. on Industrial Electronics*, 49(1):3-14.
- Zhang, H., Pan, Z.P., 2003. Nonlinear inductance mathematical model of switched reluctance generator and its application. *Small and Medium Electric Machines*, 30(3):6-9 (in Chinese).